Journal of Bio- and Tribo-Corrosion (2023) 9:52
https://doi.org/10.1007/s40735-023-00773-6

Effect of Y_2O_3 Reinforcement on Hot Corrosion of Cr_2O_3-Based Composite Coatings at Elevated Temperature

Davinder Singh[1] · Khushdeep Goyal[1] · Charanjit Singh[1] · Harvinder Singh[1]

Received: 29 March 2023 / Revised: 3 May 2023 / Accepted: 9 June 2023 / Published online: 17 June 2023

Abstract
In this research work, hot corrosion behavior of different Y_2O_3-reinforced Cr_2O_3 matrix-based composite coatings on boiler tube steel has been examined at elevated temperature. Hot corrosion tests are carried out under molten salt environment of $Na_2SO_4 + 60\%$ V_2O_5 salt mixture at 900 °C for 50 cycles. Each cycle was consisting of 1 h heating in a silicon carbide tubular furnace followed by 20 min of cooling. The coatings on samples were developed by plasma-sprayed process. The parabolic rate constants of coated steels are lower when compared to the uncoated substrate. The outcome of the experiment has indicated that highest corrosion resistance was shown by 20 wt.% Y_2O_3–Cr_2O_3, and 10 wt.% Y_2O_3–Cr_2O_3 composite coatings. The 20 wt.% Y_2O_3–Cr_2O_3, and 10 wt.% Y_2O_3–Cr_2O_3 coatings were able to reduce the corrosion rate of boiler steel by 85.58 and 83.84%, respectively, at 900 °C temperature.

Keywords Corrosion · Porosity · Coatings · Thermal spray · Boiler steel

1 Introduction

The low-grade fuels used in power plants have various impurities in them such as Na, S, K, V, and ash content [1]. These impurities play a major role in reducing the lifetime of materials, ultimately leading to deterioration of material. Such deterioration usually takes place at very high temperature (800–900 °C). Hot corrosion is a type of corrosion that occurs at high temperatures, typically above 400 °C, in the presence of molten salts or oxides. This type of corrosion is particularly prevalent in industrial applications such as gas turbines, boilers, and other high-temperature equipment [2, 3]. In India, hot corrosion is alone responsible for the loss of 6500 million US dollars [4]. Due to hot corrosion, life of components reduces and leads to shut-down of plants [5]. The contaminants released from burning of fuel are sulfur (S), sodium (Na), and chlorine (Cl). These contaminants are of corrosive nature and are responsible for the formation of gaseous environment [6–10]. In hot corrosion, material reacts with molten salt environment Na_2SO_4–60 wt.% at high elevated temperature and corrosion occurs [11]. Hot corrosion leads to formation of oxide scale. The material suffering from hot corrosion is subject maximum weight gain [12]. The process of hot corrosion is mainly of two types: (a) high-temperature hot corrosion and (b) low-temperature hot corrosion. The high-temperature hot corrosion (HTHC) is observed at high temperature between 850 and 950 °C and low-temperature hot corrosion is observed between 600 and 750 °C temperature [13]. By the use of coatings, the corrosion resistance of any component can be increased [14]. There are some other methods to protect the material from hot corrosion such as use of selective alloys, proper washing of the components, and fuel composition [15] but the use of coatings has been widely recognized by industries. Generally, composite coatings perform better to protect material from hot corrosion. Among various coating techniques, thermal sprayed techniques are used to produce dense and uniform coatings [16]. It is also confirmed by previous research studies that thermal spray techniques and reinforced coating give highest corrosion resistance.

Bhatia et al. [17] studied the hot corrosion behavior of HVOF-sprayed 75% Cr_3C_2–25% (Ni–Cr) coating on T-91boiler tube steel. From the experimental results, the coating was found useful in providing corrosion resistance. The coating showed less than 2% porosity along with dense microstructure. Mittal et al. [18] successfully deposited Cr_3C_2–NiCr and Cr_2O_3 on T-11 steel by D-Gun-sprayed

✉ Khushdeep Goyal
khushgoyal@yahoo.com

[1] Department of Mechanical Engineering, Punjabi University, Patiala, Punjab, India

technique. From the experimental results, it was found that Cr_3C_2–NiCr-coated sample showed highest corrosion resistance. Bala et al. [19] investigated the HVOF and cold-sprayed Ni–20Cr coating on ASTM-SA213-T22 steel and found the rate of corrosion was reduced by 82% and for cold-sprayed Ni–20Cr, the corrosion rate was reduced by 56%, respectively. The HVOF-sprayed Ni–20Cr coating showed higher hardness and both the coatings were able to retain their surface contact with samples. Bala et al. [20] examined the cold-sprayed Ni–50Cr and Ni–20Cr coating on T22 steel decreases the actual weight gain by 78 and 88%. Rani et al. [21] investigated the D-Gun-sprayed Cr_2O_3–50% Al_2O_3 coating on T22 boiler steel in molten salt environment Na_2SO_4–60% V_2O_5. The coated steel sample indicated less weight gain and major phases of Al and Cr were observed. These presence of these phases was the reason of hot corrosion resistance. Goyal et al. [22] investigated the performance of uncoated and HVOF-coated T22 samples exposed to a molten salt environment at 700 °C. The results showed that ASTM-SA213-T22 steel suffered from Fe_2O_3 spatter in scale. HVOF-coated T22 steel samples showed less weight and corrosion resistance.

Thermal barrier coating is a type of ceramic coating with a layer structure. It not only reduces thermal fatigue but also prevents oxidation and corrosion of the underlying metal. The current coating material (Y_2O_3) can provide significant protection for existing engines. The conventional Cr_2O_3 coating is used in the current work because Cr_2O_3 is an excellent spraying material with higher spraying deposition efficiency and the coating is less expensive with the property of tight coating bonding. The coefficient of thermal expansion of Y_2O_3 is comparable to that of nickel- and cobalt-based super alloys used for boiler components. Therefore, in this work, novel Y_2O_3-reinforced Cr_2O_3-based coatings have been developed over boiler steel and their hot corrosion behavior has been investigated in molten salt environment of Na_2SO_4–60wt% V_2O_5 at 900 °C temperature.

2 Experimental Procedure

2.1 Substrate Material

The ASME-SA213-T-91 boiler steel was used in this investigation. It was procured from the Guru Nanak Dev Thermal Power Plant at Bathinda in Punjab (India). ASME-SA213-T-91 steel alloy is commonly used in industrial boilers and also used in heat exchangers and super-heaters. The chemical composition of T-91 boiler steel is discussed in Table 1

Table 1 Composition of ASME-SA213-T-91 boiler tube steels

Elements	Nominal percentage	Actual percentage
C	0.05–0.15	0.11
Si	0.5	0.5
Mn	0.3–0.6	0.41
S	0.025	0.025
P	0.025	2.04
Cr	1.9–2.6	2.02
Mo	0.87–1.13	1.09

Table 2 Designation of coatings

Coatings	Designation	Composition (in wt.%)
Coating 1	C1	100% Cr_2O_3
Coating 2	C2	10% Y_2O_3–90% Cr_2O_3
Coating 3	C3	20% Y_2O_3–80% Cr_2O_3

2.2 Sample Preparation from Substrate Material

The samples of size 20 mm × 15 mm × 5 mm were cut from boiler tube steel. Before plasma spraying, the samples were grounded with SiC emery abrasive papers down to 180 grit and grit blasted with alumina powders (Al_2O_3-45 grit).

2.3 Development of Coatings

The coatings on the surface of T-91 boiler steel samples were deposited by Metallizing Equipment Pvt. Ltd. Jodhpur, Rajasthan. Asymmetrical shaped Cr_2O_3 (purity greater than 99.5%, particle size 15–45 µm) and Y_2O_3 (purity greater than 99.5%, particle size 15–45 µm) coating powders were mixed to prepare different types of coatings: (1) 100 wt.% Cr_2O_3 (2) 10% Y_2O_3–90% Cr_2O_3 and (3) 20% Y_2O_3–80% Cr_2O_3. These coatings were developed by plasma spray technique. The spray parameters employed were as follows:

- Current 550 A
- Voltage 50 V
- Arc pressure (primary gas) 65 PSI
- Carrier gas pressure 50 PSI
- Hopper RPM 6
- Hydrogen (secondary gas) 12 PSI

Table 2 shows designations of coatings used.

2.4 High-Temperature Investigations at 900 °C

The study of hot corrosion for uncoated and coated T-91 boiler steels was conducted at 900 °C temperature in the molten salt environment Na_2SO_4–60 wt.% V_2O_5. Molten salt Na_2SO_4–60 wt.% V_2O_5 was selected to carry out the present research because vanadium (V) and sodium (Na) are the contaminants usually present in low-grade fuels. The bare T-91 sample was firstly, mirror polished and after that, the dimension of sample was measured by using digital vernier caliper. The weight of each sample was measured before every cycle. The furnace temperature was also remained same throughout the process, i.e., 900 °C. The samples were kept in furnace individually for 1 h and which is followed by 20 min air cooling. After every cycle, the weight of the sample was measured by electronic weighing machine. The same was repeated for the total of 50 cycles. The corroded products were investigated using SEM, EDS, and X-ray diffraction methods to determine the composition and microstructure.

3 Results

3.1 Visual Inspection

The macrographs of uncoated and coated T-91 samples are shown in Fig. 1. The macrograph of uncoated T-91 sample is shown in Fig. 1a. The reddish-brown color was observed on uncoated T-91 boiler steel. Spallation and increase in corrosion were also observed. Figure 1b shows the C1 coating on T-91 boiler steel which indicated gray-black patches on the surface of sample. Figure 1c, d shows the micrographs of C2 and C3 coatings which indicated that there were no cracks on the surface of sample. Small scales were also observed.

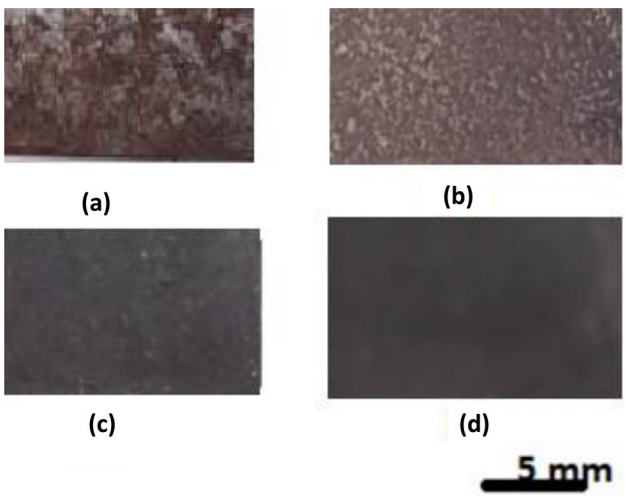

Fig. 1 Macrographs of plasma-sprayed T-91sample **a** uncoated T-91, **b** C1-coated, **c** C2-coated, **d** C3-coated samples

3.2 Coating Thickness and Porosity

The thicknesses of the coatings were monitored during the spraying process to obtain the coatings of uniform thickness. A Minitest-2000 thin film thickness gauge (Make: Elektro-Physik Koln Company, Germany, precision ± 1 µm) was used to monitor the thickness of each developed coating. The average thickness of the coatings was measured from the BSE images and is compiled in Table 3. Measurements of the porosity of the coated and uncoated samples were done with an image analyser, having software of the Envision 3.0 Series (Chennai Metco Private Limited, Chennai, India). The average thickness of the coatings and porosity values are displayed in Table 3.

3.3 Change in Weight

Cumulative weight gain of all uncoated and coated samples for all 50 cycles is shown in Fig. 2, whereas Fig. 3 shows cumulative weight gain after 50 cycles of exposure to elevated temperature. After 20th cycle, the weight gain of C1-coated T-91 sample was increased. In case of Y_2O_3-reinforced Cr_2O_3 coatings, the rate of weight gain kept on decreasing. For C1-coated T-91 sample, the cumulative weight gain was 44.60 mg-cm^{-2}. Thus, it can be observed that the weight gain reduced by C1-coated sample is 59.98%. In C2 coating (10 wt.% Y_2O_3–Cr_2O_3) at 900 °C, the weight gain was further reduced at 900 °C. The weight gain observed for C2 and C3 coatings was 18.15 and 16.20 mg-cm^{-2}, respectively. The weight gain of C2 and C3 coatings was reduced by 83.84 and 85.58%, respectively, as compared to that of uncoated sample. Overall, it was found that C3 coating showed the maximum resistance to corrosion.

3.4 SEM/EDS Analysis

The SEM analysis for T-91 uncoated and coated T-91 samples is shown in Fig. 4. For uncoated sample, the SEM analysis is shown in Fig. 4a. The uncoated T-91 boiler steel sample surface was in direct contact of molten salt environment Na_2SO_4–60% V_2O_5. The oxide scales were developed on its surface and had irregular size of flakes. The EDS analysis for uncoated T-91 sample is shown in Fig. 5a. The EDS analysis indicated the presence of Fe and O scale. The SEM analysis

Table 3 Coating thickness and porosity

Coatings	Coating thickness (µm)	Porosity (%)
Coating 1	250	2.05
Coating 2	255	1.87
Coating 3	250	1.68

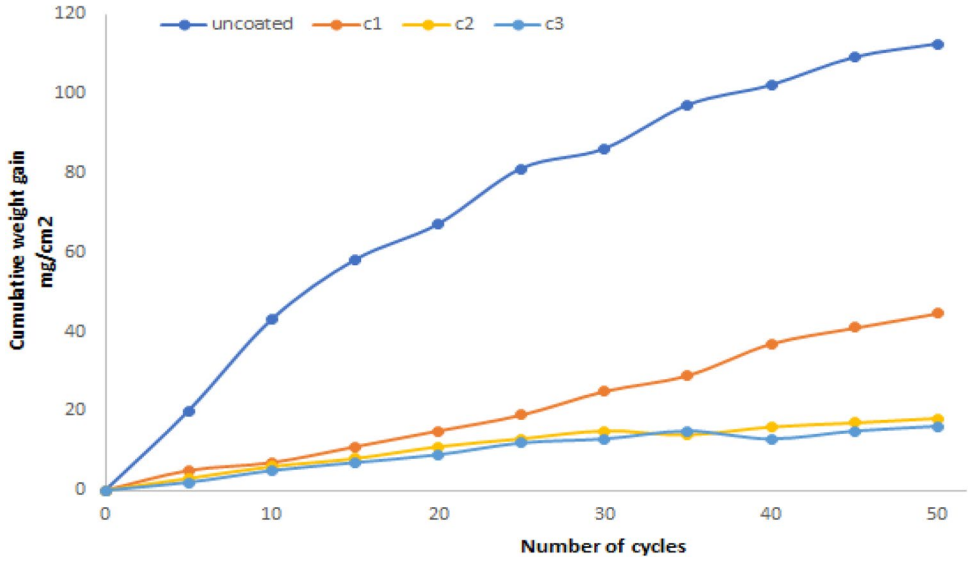

Fig. 2 Cumulative weight gain vs number of cycles for **a** T-91 uncoated and C1-, C2-, C3-coated samples

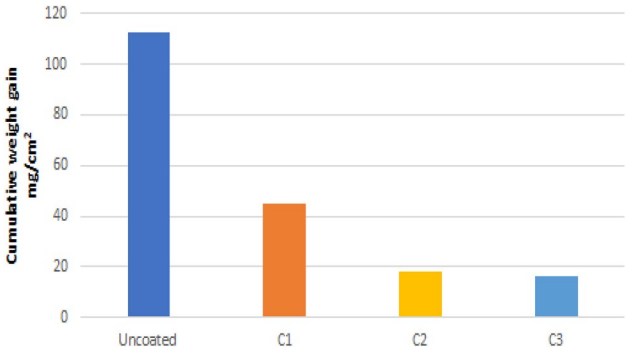

Fig. 3 Cumulative weight gain for T-91 uncoated and C1-, C2-, C3-coated T-91 samples

for C1-coated T-91 sample is shown in Fig. 4b. It showed the contamination of Cr and Fe oxides and it was confirmed by the EDS analysis (Fig. 5b). The SEM image of C2-coated T-91 sample indicated very less corrosion as compared to uncoated T-91 and C1-coated samples. SEM analysis of C2-coated T-91 sample showed dense scale as can be seen in Fig. 4c. SEM analysis for C3-coated T-91 sample is shown in Fig. 4d. The corrosion rate of C3 coated was very less as compared to all the coated samples. The dense surface morphology was observed for C3-coated sample. The EDS analysis for C2- and C3-coated T-91 sample indicated the rich presence of Y and Cr in coating microstructure as can be seen in Fig. 5c, d.

3.5 XRD Analysis

The XRD analysis for Bare T-91 boiler steel in molten salt environment Na_2SO_4–60% V_2O_5 is shown in Fig. 6a. The XRD analysis indicated the formation of Fe_2O_3 as the major constituent along with the peaks of Cr_2O_3 as depicted by Fig. 6a. The XRD analysis for plasma-sprayed C1-coated T-91 sample in molten salt environment is shown in Fig. 6b. Major peaks of Cr_2O_3 phases were observed which helps to develop the resistance against hot corrosion. Minor peaks of Na_2O were also observed. XRD spectra for C2 coating reveal the Y_2O_3 as prominent phase (Fig. 6c). For C3 coating, major peaks indicated the presence of element Y_2O_3 and minor peaks of Cr_2O_3 (Fig. 6d).

4 Discussion

The different Y_2O_3-reinforced Cr_2O_3 coatings were deposited successfully on T-91 boiler steel with the help of plasma-sprayed process. The porosity of Cr_2O_3 coatings was reduced with the increase in Y_2O_3 content. The reduction in porosity value of plasma-sparyed coatings was due to the low process temperature during thermal spraying process, which might have resulted in minimal shrinkage upon cooling [11]. It was observed from this research work that all coated samples of T-91 steel have provided better result in terms of corrosion resistance as compared to T-91 uncoated sample. Uncoated T-91 sample showed immense surface spalling. During the hot corrosion studies, the corrosion rate of uncoated sample increased at a comparatively higher rate during the initial cycles, possibly because of the formation of cracks in the oxide scale. It was found that the weight gain was continuously increasing after the first cycle due to the quick formation of Fe_2O_3 scale. This scale was of porous nature and it was formed due to hot corrosion. The change in color was also noticed after 8th cycle and a red rusty color appeared on the surface of T-91. After 10th cycle, red rusty color was changed into brown color. The EDS analysis of

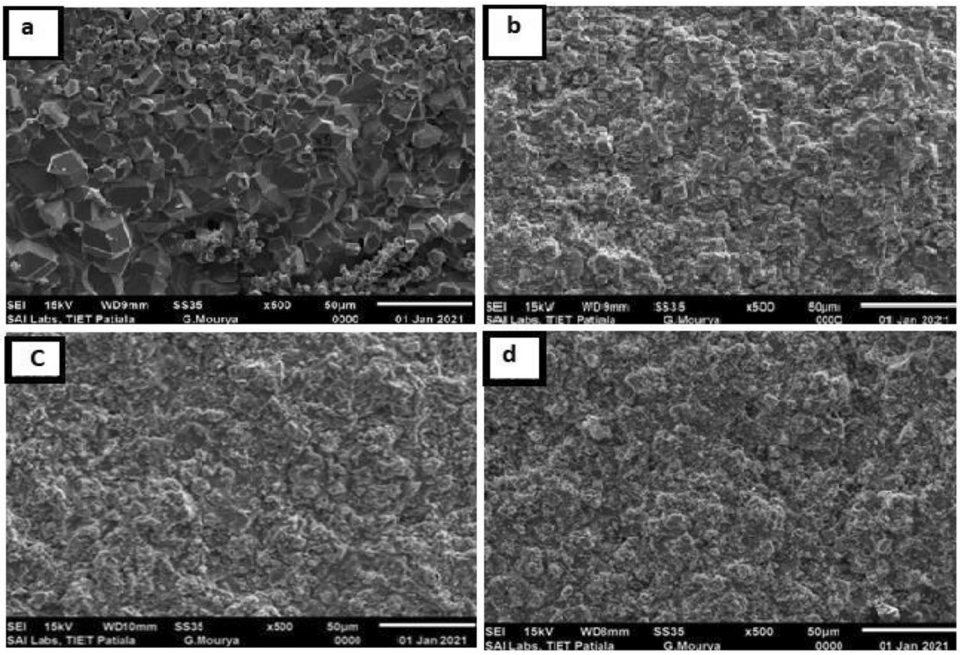

Fig. 4 SEM micrograph for **a** T-91 uncoated (irregular flakes of Fe_2O_3), **b** C1-coated (irregular splats with small voids), **c** C2-coated (dense and uniform coating), **d** C3-coated T-91 boiler steel (dense and uniform coating)

uncoated T-91 steel at 900 °C showed the development of white and gray region on the surface of material and presence of C, O, Si, and Fe elements was observed. Fe_2O_3 during hot corrosion experiments in a molten salt environment has also been reported by Goyal et al. [22], Rani et al. [23], and Singh et al. [24]. Further, the uncoated T-91 sample was subjected to EDS analysis and this analysis showed the presence of Fe and O as these were major elements formed on the surface of T-91 uncoated sample. Sample of T-91 steel coated with Cr_2O_3 showed better adherence quality which is the characteristic of the plasma spray thermal process [25, 26]. Formation of less Fe_2O_3 was confirmed from the XRD graph of T-91 Cr_2O_3-coated steel. The aggressive species, primarily O^{2-} formed as a result of the dissolution of Na_2SO_4, interacts with the superior layer of the coating and begins to penetrate over the coating boundary due to hot corrosion, which might be the reason of formation of Fe_2O_3 in Cr_2O_3-coated steel [25, 27, 28]. The cumulative weight gain graph for Cr_2O_3-coated T-91 sample showed the reduction in weight gain by 44.60 mg/cm^2 which revealed that the reduction in corrosion by 60.03%. The SEM micrographs indicated a nodular structure with gray and white contrast phases, which might be due to the oxides of chromium and iron in the scale. The positive corrosion resistance could improve because of the reaction of Cr_2O_3, which stabilized the melt chemistry by developing Na_2CrO_4 solute and inhibited the dissolution of the protective oxide scale [26, 29]. Microcracking of the scale occurred due to the presence of different thin-layer phases, which might impose severe strain on the coatings [30].

The results of cumulative weight gain showed that the corrosion resistance was maximum in 20 wt.% Y_2O_3–Cr_2O_3 followed by 10wt.% Y_2O_3–Cr_2O_3-reinforced coating. The rate of corrosion was reduced by 83.34 and 85.58%, respectively. The cumulative weight gain of 20 wt.%Y_2O_3-Cr_2O_3 reinforced was found to be minimum, i.e., 16.20 mg/cm^2. The cumulative weight gain for 10 wt.% Y_2O_3–Cr_2O_3-reinforced coating also showed minimum weight gain, i.e., 18.15 mg/cm^2. The coated samples of T-91 steel were very successful to hold the attack of corrosion and with the help of weight gain graphs. it can be confirmed that Y_2O_3–Cr_2O_3-coated sample of T-91 steel was good to handle the corrosion attack. The pores in the chromium oxide formed along the boundaries of the coating and Y plasma spray splats channels allowed the coatings to grow walls against the diffusion and penetration of corrosive elements. The $Y_2O_3 + Cr_2O_3$ coating's superior corrosion resistance at higher temperatures could be attributed to its extremely low porosity. Because the coatings developed have a dense and flat splat structure, the distance from the substrate to the coating interface along the splat boundaries increases significantly, giving the coatings excellent corrosion resistance. The ability of withstand hot corrosion enhanced due to addition of Y_2O_3 in the coating matrix [31–33]. As the reaction progresses, elements such as Y oxidize at the upper surface of the coating, while chromium oxidizes into chromium oxide. Thus, chromium oxide (Cr_2O_3) forms a continuous layer and provides excellent corrosion resistance. The addition of Y_2O_3 significantly improves the coating's corrosion resistance, owing to grain refinement. The grain boundary is in a high energy state with a high number of dislocations

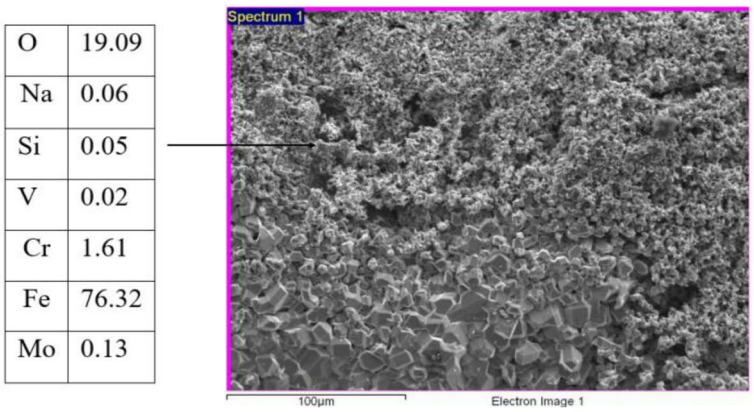

(a)

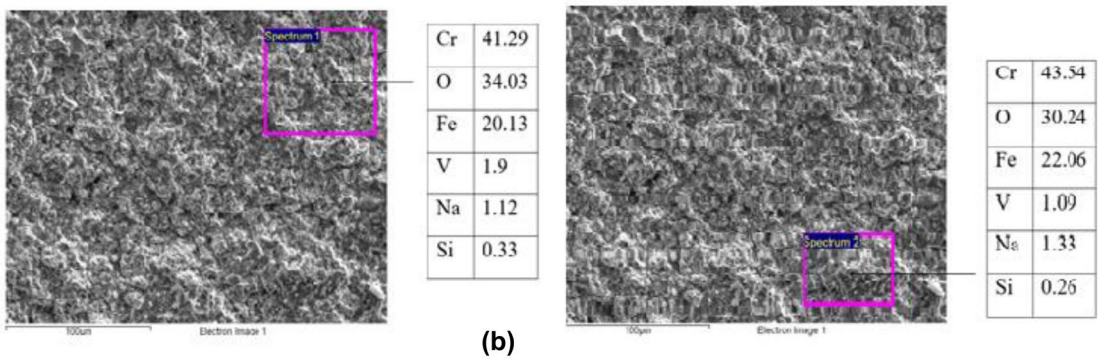

(b)

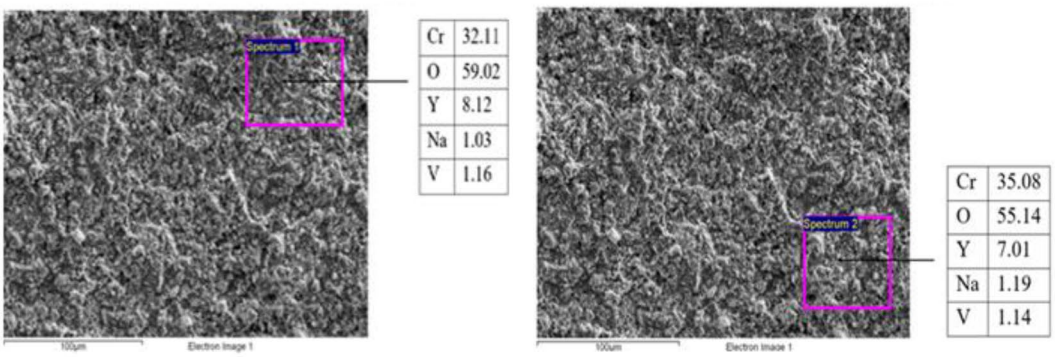

(c)

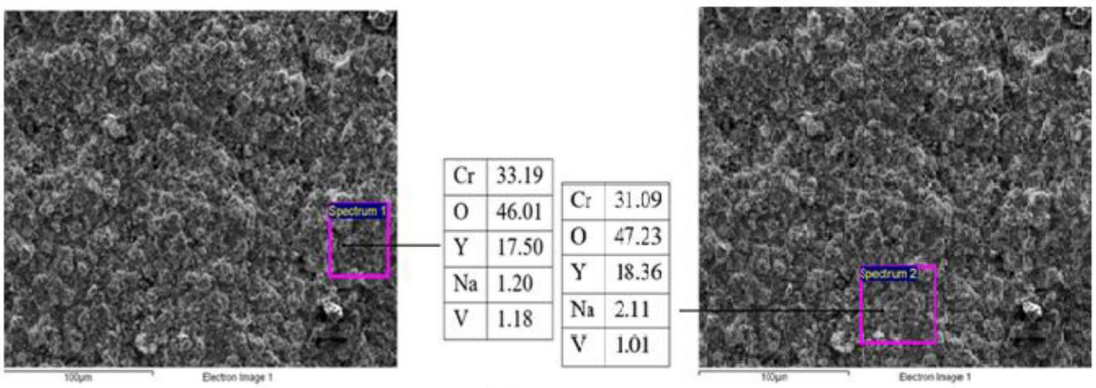

(d)

Fig. 5 **a** EDS analysis for uncoated T-91 sample. **b** EDS analysis for C1-coated T-91 sample. **c** EDS analysis for C2-coated T-91 sample. **d** EDS analysis for C3-coated T-91 sample

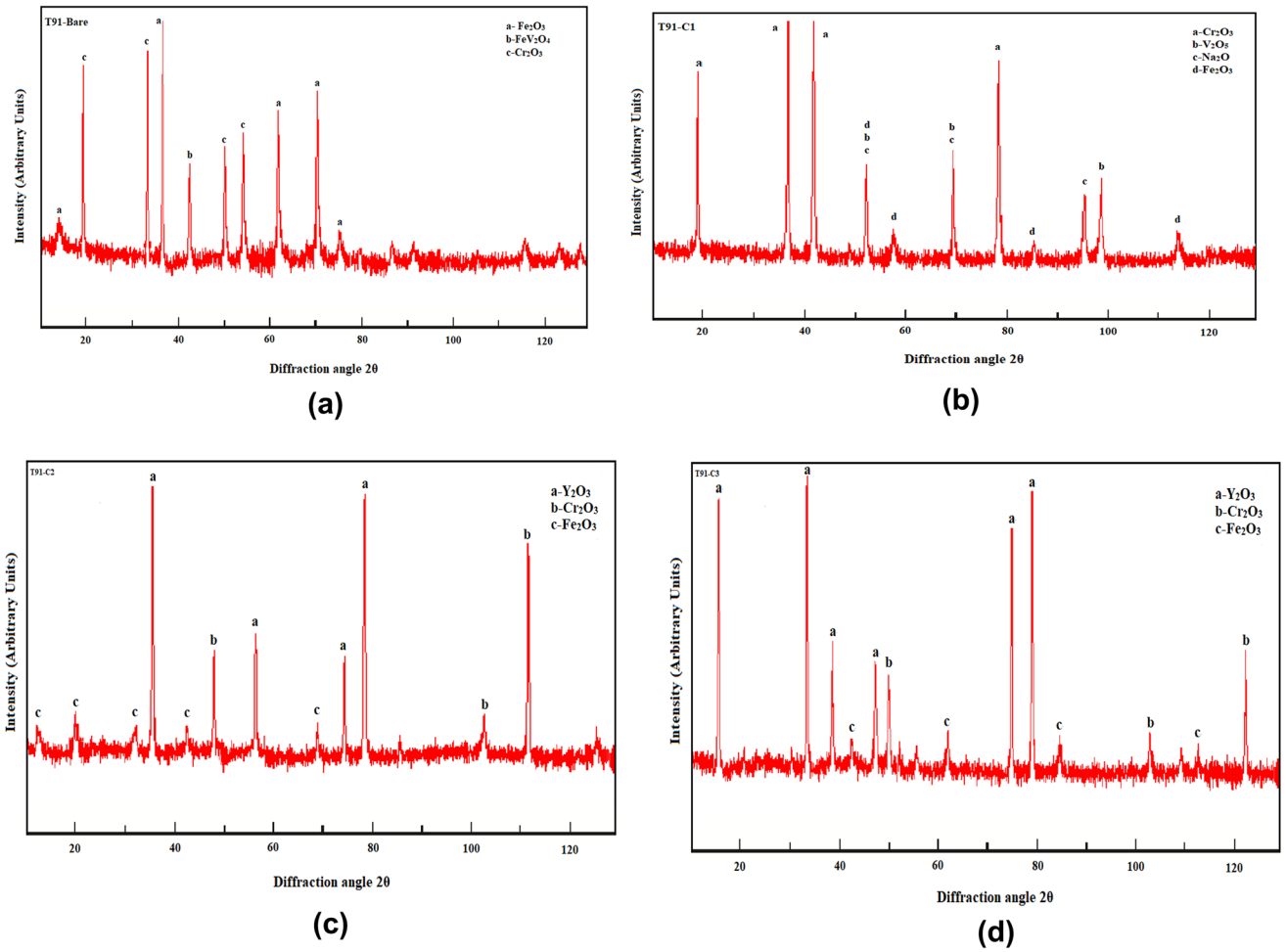

Fig. 6 **a** XRD analysis for uncoated T-91 sample. **b** XRD analysis for C1-coated T-91 sample. **c** XRD analysis for C2-coated T-91 sample. **d** XRD analysis for C3-coated T-91 sample

and defects, and the fine-grained structure provides more active sites for passivation film nucleation and growth [34, 35]. Further, the top layer consisted of Y_2O_3 and Cr_2O_3 on surface, which efficiently had slowed down the diffusion rate of oxygen leading to increase in corrosion resistance of composite coatings. The SEM analysis of T-91 steel coated with 20 wt.% Y_2O_3–Cr_2O_3 showed the working ability of this coating at high temperature as there were no voids found on the surface of the sample. The T-91 sample coated with 20wt.%Y_2O_3-Cr_2O_3 showed the lowest weight gain. The EDS analysis of 20 wt.% Y_2O_3–Cr_2O_3 coating showed the presence of Y, Cr, Y_2O_3, Fe_2O_3, Cr_2O_3, and the XRD analysis of Cr_2O_3 coating showed the presence of V_2O_5, Cr_2O_3, and Fe_2O_3.. The existence of Cr, Fe, V, Na, and O was confirmed by the EDS over the coating surface. Therefore, the Cr_2O_3–Y_2O_3 composite coating could improve the oxidation resistance of boiler steel alloy at elevated temperatures.

5 Conclusions

1. The uncoated T-91 sample showed highest corrosion rate and minimum resistance to corrosion at high temperature.
2. In uncoated T-91 sample, Fe_2O_3 was observed as major phase in molten salt environment of Na_2SO_4–60 wt.% V_2O_5 by XRD analysis.
3. The cumulative weight gain was minimum for 20 wt.% Y_2O_3–Cr_2O_3 composite coating and was found to be 16.20 mg/cm^2.
4. The T-91 sample coated with 20 wt.% Y_2O_3–Cr_2O_3 showed the least corrosion rate and maximum resistance to corrosion at high temperature. This composite coating was able to reduce the corrosion rate of uncoated steel by 85.58%.

5. The coatings used on ASME-SA213-T-91 at 900 °C in molten salt environment were found out to be corrosion resistant. The order of corrosion resistance for the applied coatings on T-91 was

   20 wt.% $Y_2O_3 - Cr_2O_3$ > 10 wt.% $Y_2O_3 - Cr_2O_3$ > Cr_2O_3 > Bare.

Author Contributions DS and KG contributed to conception of work, experimental design, experimentation, data analysis, and draft of manuscript. CS and HS contributed to experimentation, dara analysis, and manuscript draft.

Funding Authors declare that they have not received any funding from any source.

Availability of Data and Materials All data have been included in this manuscript.

Declarations

Conflict of interest Authors declare that they have no conflict of interest, and they have also no financial interest.

Ethical approval Not applicable.

References

1. El Rayes MM, Abdo HS, Khalil KA (2013) Erosion–corrosion of cermet coating. Int J Electrochem Sci 8(1):1117–1137
2. Garip Y (2022) An investigation on the corrosion performance of $Fe_2CoCrNi0.5$ based high entropy alloys. Corros Sci 206:110497
3. Garip Y, Garip Z, Ozdemir O (2020) Prediction modeling of Type-I hot corrosion performance of Ti–Al–Mo–X (X= Cr, Mn) alloys in (Na, K) $2SO_4$ molten salt mixture environment at 900 °C. J Alloy Compd 843:156010
4. Singh J, Vasudev H, Singh S (2020) Performance of different coating materials against high temperature oxidation in boiler tubes—a review. Mater Today Proc 26:972–978
5. Goyal DK, Singh H, Kumar H, Sahni V (2012) Slurry erosive wear evaluation of HVOF-spray Cr_2O_3 coating on some turbine steels. J Therm Spray Technol 21:838–851
6. Levy AV (1993) The erosion–corrosion of tubing steels in combustion boiler environments. Corros Sci 35(5–8):1035–1043
7. Chawla V, Chawla A, Puri D, Prakash S, Gurbuxani PG, Sidhu BS (2011) Hot corrosion & erosion problems in coal based power plants in India and possible solutions—a review. J Miner Mater Charact Eng 10(04):367
8. Kumar N, Kanwar R (2012) To study erosion behavior of Cr. Int J Emerg Technol 3(1):69–73
9. Garg BP, Kumar N (2013) Protection of SAE 213 T-22 boiler steel tube material with various power coatings using HVOF spray technique. J Environ Nanotechnol 2:30–36
10. Huttunen-Saarivirta E, Stott FH, Rohr V, Schütze M (2007) Erosion-oxidation behavior of chromized-aluminized 9% chromium steel under fluidized-bed conditions at elevated temperature. Oxid Met 68:113–132
11. Kamal S, Jayaganthan R, Prakash S, Kumar S (2008) Hot corrosion behavior of detonation gun sprayed Cr_3C_2–NiCr coatings on Ni and Fe-based superalloys in Na_2SO_4–60% V_2O_5 environment at 900 °C. J Alloy Compd 463(1–2):358–372
12. Singh H, Puri D, Prakash S (2005) Some studies on hot corrosion performance of plasma sprayed coatings on a Fe-based superalloy. Surf Coat Technol 192(1):27–38
13. Mannava V, Rao AS, Paulose N, Kamaraj M, Kottada RS (2016) Hot corrosion studies on Ni-base superalloy at 650 °C under marine-like environment conditions using three salt mixture (Na_2SO_4+ NaCl+ $NaVO_3$). Corros Sci 105:109–119
14. Pawlowski L (2008) The science and engineering of thermal spray coatings. Wiley, New York
15. Singh A, Goyal K, Goyal R, Krishan B (2021) Hot corrosion behaviour of different ceramics coatings on boiler tube steel at 800 °C temperature. J Bio-and Tribo-Corros 7:1–9
16. Goyal A, Singh R, Singh G (2017) Study of high-temperature corrosion behavior of D-Gun spray coatings on ASTM-SA213, T-11 steel in molten salt environment. Mater Today Proc 4(2):142–151
17. Bhatia R, Singh H, Sidhu BS (2014) Hot corrosion studies of HVOF-sprayed coating on T-91 boiler tube steel at different operating temperatures. J Mater Eng Perform 23:493–505
18. Mittal R, Singh H (2020) Evaluation of the behavior of D-Gun sprayed coatings on T-11 boiler steel at 900 °C temperature. Mater Today Proc 26:549–555
19. Bala N, Singh H, Prakash S, Karthikeyan J (2012) Investigations on the behavior of HVOF and cold sprayed Ni–20Cr coating on T22 boiler steel in actual boiler environment. J Therm Spray Technol 21:144–158
20. Bala N, Singh H, Karthikeyan J, Prakash S (2013) Performance of cold sprayed Ni–20Cr and Ni–50Cr coatings on SA 516 steel in actual industrial environment of a coal fired boiler. Mater Corros 64(9):783–793
21. Rani A, Bala N, Gupta CM (2017) Accelerated hot corrosion studies of D-Gun-sprayed Cr_2O_3–50% Al_2O_3 coating on boiler steel and Fe-based superalloy. Oxid Met 88:621–648
22. Goyal K, Singh H, Bhatia R (2019) Hot-corrosion behavior of Cr_2O_3-CNT-coated ASTM-SA213-T22 steel in a molten salt environment at 700 °C. Int J Miner Metall Mater 26:337–344
23. Rani A, Bala N, Gupta CM (2017) Characterization and hot corrosion behavior of D-Gun sprayed Cr_2O_3–75% Al_2O_3 coated ASTM-SA210-A1 boiler steel in molten salt environment. Anti-Corros Methods Mater 64(5):515–528
24. Singh S, Goyal K, Goyal R (2016) Performance of Cr_3C_2–25 (Ni–20Cr) and Ni–20Cr coatings on T91 boiler tube steel in simulated boiler environment at 900 °C. Chem Mater Eng 4(4):57–64
25. Ullah I, Siddiqui MA, Liu H, Kolawole SK, Zhang J, Zhang S et al (2020) Mechanical, biological, and antibacterial characteristics of plasma-sprayed (Sr, Zn) substituted hydroxyapatite coating. ACS Biomater Sci Eng 6(3):1355–1366
26. Yang X, Dong S, Zeng J, Zhou X, Jiang J, Deng L, Cao X (2019) Sliding wear characteristics of plasma-sprayed Cr_2O_3 coatings with incorporation of metals and ceramics. Ceram Int 45(16):20243–20250
27. Singh S, Goyal K, Bhatia R (2022) A review on protection of boiler tube steels with thermal spray coatings from hot corrosion. Mater Today Proc 56(1):379–383
28. Parkash J, Saggu HS, Vasudev H (2022) A short review on the performance of high velocity oxy-fuel coatings in boiler steel applications. Mater Today Proc 50:1442–1446
29. Patil VG, Somasundaram B, Kandaiah S, Kumar S (2022) High temperature corrosion behavior of high velocity oxy fuel sprayed NiCrMoFeCoAl-30% SiO_2 and NiCrMoFeCoAl-30% Cr_2O_3 composite coatings on ASTM SA213-T22 steel in a coal-fired boiler environment. Int J Eng 35(7):1416–1427

30. Goyal K, Singh H, Bhatia R (2018) Cyclic high temperature corrosion studies of carbon nanotubes-Cr_2O_3 composite coatings on boiler steel at 900 °C in molten salt environment. Anti-Corros Methods Mater 65(6):646–657
31. Ozkan D (2023) Structural characteristics and wear, oxidation, hot corrosion behaviors of HVOF sprayed Cr_3C_2–NiCr hardmetal coatings. Surf Coat Technol 457:129319
32. Garip Y, Ozdemir O (2019) Comparative study of the oxidation and hot corrosion behaviors of TiAl–Cr intermetallic alloy produced by electric current activated sintering. J Alloy Compd 780:364–377
33. Garip Y, Ozdemir O (2020) Corrosion behavior of the resistance sintered TiAl based intermetallics induced by two different molten salt mixture. Corros Sci 174:108819
34. Zhang Y, Wu H, Yu X, Tang D (2022) Role of Cr in the high-temperature oxidation behavior of Cr_xMnFeNi high-entropy alloys at 800 °C in air. Corros Sci 200:110211
35. Cui C, Wu M, Miao X, Zhao Z, Gong Y (2022) Microstructure and corrosion behavior of CeO_2/FeCoNiCrMo high-entropy alloy coating prepared by laser cladding. J Alloy Compd 890:161826